

# Preparation of Monolithic Carbon Aerogels and Investigation of Their Pore Interconnectivity by a Nanocasting Pathway

Wen-Cui Li, An-Hui Lu, and Ferdi Schüth\*

Max-Planck-Institut für Kohlenforschung, D-45470 Mülheim, Germany

Received February 16, 2005. Revised Manuscript Received April 19, 2005

Monolithic carbon aerogels have been prepared using magnesium acetate as catalyst based upon a polycondensation of resorcinol with formaldehyde and an ambient pressure drying followed by carbonization. Carbon aerogels have been synthesized with different catalyst concentration and solid content. The structure of the different aerogels has been investigated in detail by nitrogen sorption measurements, scanning electron microscopy (SEM), and transmission electron microscopy (TEM). The surface areas of such carbon aerogels result from the contributions of both mesopores and micropores. The contribution of the micropores to total pore volume is higher than that of samples synthesized with the conventionally used sodium carbonate as catalyst. If a saturated solution of magnesium hydroxide was used as catalyst, the synthesized carbon aerogels almost exclusively consist of micropores and macropores, exhibiting a hierarchical structure. Using the as-prepared carbon aerogels as hard templates, porous silica monoliths can be created by a nanocasting pathway. This demonstrates that carbon aerogels synthesized with  $\text{Mg}^{2+}$  as catalyst during the sol–gel process exhibit robust frameworks and improved pore interconnectivity.

## 1. Introduction

Ordered mesoporous inorganic materials have attracted intensive attention since the first appearance of the M41S family which was described by scientists of the Mobil Oil Corporation in 1992,<sup>1</sup> although less ordered mesoporous solids, such as silica gels or carbons, had been known for decades before this discovery. They can be widely used in large-scale processes in the chemical and petrochemical industry as adsorbents, catalysts, supports, as well as for many other uses.<sup>2,3</sup> The most often used method to fabricate ordered mesoporous materials is the use of surfactant supramolecular arrays as templates, as in the synthesis of the SBA-*n* series.<sup>4</sup> Recently, the hard templating or nanocasting route, using either mesoporous silica or carbon as template, was introduced as a possibly more flexible pathway to create mesoporous materials with any desired composition, as long as the precursor solutions can be introduced into the pore system of the template and the formed solid is stable during the template removal process.<sup>5–10</sup> However, these mesoporous materials usually are formed as fine powders,

which in a reactor would give rise to excessive pressure drops in practical application.<sup>11</sup> To prevent this, the fine powders are commonly agglomerated into granules using inert binders such as clay minerals, silica, and other materials. Nevertheless, the use of binders can lead to new problems, such as pore blocking, diffusion limitations, and lowering of the concentration of active material. To overcome such problems associated with mesoporous powder materials, developing a synthetic method to directly fabricate three-dimensionally connected porous materials in monolithic form seems desirable. If the nanocasting route is to be used, a porous monolithic template is necessary in order to obtain a replica with monolithic shape. A porous silica monolith has been used as a template to prepare monolithic carbon with a hierarchical structure through a nanocasting pathway by Lindén et al.<sup>12</sup>

Carbon aerogels represent a class of monolithic mesoporous materials with high surface area and high pore volume as well as controllable pore structures;<sup>13</sup> these materials are expected to be commercially used as catalyst supports,<sup>14</sup> electrode materials for electric double-layer capacitors,<sup>15</sup> and in many other promising applications. Generally, carbon aerogels are produced through a sol–gel process, using the polycondensation of resorcinol with formaldehyde in the presence of a tiny amount of sodium carbonate, and subsequently followed by supercritical drying,<sup>13</sup> ambient

\* To whom correspondence should be addressed. Fax: +49-208 306 2995. E-mail: schueth@mpi-muelheim.mpg.de.

- (1) Kresge, C. T.; Leonowicz, M. E.; Roth, W. J.; Vartuli, J. C.; Beck, J. S. *Nature* **1992**, 359, 710.
- (2) Ciesla, U.; Schüth, F. *Microporous Mesoporous Mater.* **1999**, 27, 131.
- (3) Ying, J. Y.; Mehnert, C. P.; Wong, M. S. *Angew. Chem., Int. Ed.* **1999**, 38, 56.
- (4) Zhao, D.; Feng, J.; Huo, Q.; Melosh, N.; Fredrickson, G. H.; Chmelka, B. F.; Stucky, G. D. *Science* **1998**, 279, 548.
- (5) Ryoo, R.; Joo, S. H.; Jun, S. J. *Phys. Chem. B* **1999**, 103, 7743.
- (6) Lu, A.-H.; Schmidt, W.; Taguchi, A.; Spliethoff, B.; Tesche, B.; Schüth, F. *Angew. Chem., Int. Ed.* **2002**, 41, 3489.
- (7) Yang, H.; Shi, Q.; Tian, B.; Lu, Q.; Gao, F.; Xie, S.; Fan, J.; Yu, C.; Tu, B.; Zhao, D. *J. Am. Chem. Soc.* **2003**, 125, 4724.
- (8) Schwickardi, M.; Johann, T.; Schmidt, W.; Schüth, F. *Chem. Mater.* **2002**, 14, 3913.
- (9) Schüth, F. *Angew. Chem., Int. Ed.* **2003**, 42, 3604.

- (10) Wang, Y.; Yang, C.-M.; Schmidt, W.; Spliethoff, B.; Bill, E.; Schüth, F. *Adv. Mater.* **2005**, 17, 53.
- (11) Lee, Y. J.; Lee, J. S.; Park, Y. S.; Yoon, K. B. *Adv. Mater.* **2001**, 13, 1259.
- (12) Taguchi, A.; Smått, J.-H.; Lindén, M. *Adv. Mater.* **2003**, 15, 1209.
- (13) Pekala, R. W. *J. Mater. Sci.* **1989**, 24, 3221.
- (14) Moreno-Castilla, C.; Maldonado-Hódar, F. J.; Rivera-Utrilla, J.; Rodríguez-Castellón, E. *Appl. Catal. A* **1999**, 183, 345.
- (15) Li, W.; Reichenauer, G.; Fricke, J. *Carbon* **2002**, 40, 2955.

pressure drying<sup>16</sup> or freeze-drying,<sup>17</sup> and carbonization. The nanostructures and properties of carbon aerogels are mainly determined by various synthetic and processing conditions. This leads to a remarkable potential for designing and controlling these materials to meet specific applications. Overall, the carbon aerogels undergo three main steps during their synthesis: formation of the wet gel, drying, and carbonization. During the first step, the framework of the carbon aerogels is formed through cross-linking of the reactant monomers. During the drying, the initially formed network structure should be maintained as well as possible, and the same holds for the carbonization step, where ideally the polymer framework is converted to carbon without changes in the pore structure. Hence, the primary influence on the structure of carbon aerogels can be exerted in the first step, in which the catalyst and its concentration as well as the solid content in the solution are usually the critical factors. Sodium carbonate is one of the most often used catalysts. Many other catalysts, including transition-metal catalysts such as Pt, Pd, Ag, Fe, Co, Cr, Cu, and others, have also been studied in order to control and to improve the porous structure of the resultant carbon aerogels. The nature of the metal species has a strong influence on the fine structure of carbon aerogels. The presence of Cr and Fe can promote the graphitization of the structure of the carbon aerogels.<sup>18</sup> Tungsten-doped carbon aerogels show a needlelike morphology, relatively high surface area, and large pore volume as well as high activity in acid-catalyzed reactions.<sup>19</sup>

From the viewpoint of template synthetic approaches, carbon aerogels with high surface area, large pore volume, as well as an open pore system could be used as a hard template to create porous materials. Especially the monolithic form of carbon aerogels would possibly allow the preparation of various monolithic porous materials, if the carbon aerogels possess substantial connectivity throughout the entire pore system. Kaneko and co-workers have synthesized monolithic zeolites using carbon aerogel templates which were prepared with sodium carbonate as catalyst via the supercritical drying process.<sup>20</sup> The obtained zeolite particles exhibit irregular shape and small-sized grains. As is well-known, carbon aerogels synthesized through supercritical drying have well-developed porosity and pore interconnectivity.<sup>13,20</sup> However, supercritical drying is a complex process, and usually the monolithic shapes break down if an aqueous solution is impregnated into such carbon aerogels. This is due to the pressures developed (the reason supercritical drying after the synthesis is used in the first place) as well as the flimsy skeleton of these carbon aerogels, leading to the collapse of the pore structure. Therefore, to obtain a replica with a controlled shape, it is important that the template carbon aerogels possess rigid skeletons and well-interconnected pores. To meet this demand, we have studied alternative

**Table 1. Synthetic Conditions and Texture Parameters of Carbon Aerogels and the Silica Replicas**

sample	catalyst	$S_{\text{BET}}$ $\text{m}^2 \text{g}^{-1}$	$V_{\text{mic}}$ $\text{cm}^3 \text{g}^{-1}$	$V$ $\text{cm}^3 \text{g}^{-1}$	$V_{\text{mic}}/V$
CA30/50 <sup>a</sup>	Mg(Ac) <sub>2</sub>	664	0.17	0.78	0.22
CA30/100	Mg(Ac) <sub>2</sub>	671	0.18	0.73	0.25
CA30/200	Mg(Ac) <sub>2</sub>	706	0.21	0.71	0.30
CA30/500	Mg(Ac) <sub>2</sub>	593	0.22	0.41	0.54
CA40/50	Mg(Ac) <sub>2</sub>	723	0.14	1.09	0.13
CA40/100	Mg(Ac) <sub>2</sub>	718	0.16	1.02	0.16
CA40/200	Mg(Ac) <sub>2</sub>	697	0.15	0.93	0.16
CA40/500	Mg(Ac) <sub>2</sub>	784	0.23	0.83	0.28
CA25-Mg(OH) <sub>2</sub>	Mg(OH) <sub>2</sub>	538 <sup>b</sup>	0.24	0.26	0.92
CA40-Mg(OH) <sub>2</sub>	Mg(OH) <sub>2</sub>	535 <sup>b</sup>	0.23	0.25	0.92
CA30/500-Na <sub>2</sub> CO <sub>3</sub>	Na <sub>2</sub> CO <sub>3</sub>	697	0.14	1.14	0.12
CA40/500-Na <sub>2</sub> CO <sub>3</sub>	Na <sub>2</sub> CO <sub>3</sub>	722	0.15	1.35	0.11
CA-NO	no	433 <sup>b</sup>	0.19	0.20	0.95
Silica-1		313	0.07	0.17	0.41
Silica-2		585	0.08	1.09	0.07

<sup>a</sup> Sample number CA30/50 means this sample was synthesized at 30 wt % of solid content (percentage of resorcinol and formaldehyde) and 50 of catalyst ratio (molar ratio of resorcinol/catalyst). Others represent the same meaning. CA25-Mg(OH)<sub>2</sub> and CA40-Mg(OH)<sub>2</sub> were catalyzed by Mg(OH)<sub>2</sub>-saturated solution under varied solid content.  $S_{\text{BET}}$ : specific surface area calculated on the basis of the BET method;  $V_{\text{mic}}$ : micropore volume calculated from the  $\alpha_s$ -plot method;  $V$ : total pore volume;  $V_{\text{mic}}/V$ : ratio between micropore volume and total pore volume, reflecting the fraction of the mesopore volume in the materials. <sup>b</sup> Values should be interpreted with care, since the BET algorithm is not appropriate for microporous materials.

catalysts and found that, in the presence of Mg<sup>2+</sup> during the sol-gel process, very stable structures could be synthesized. In addition, the pore interconnectivity of the resulting aerogels was determined by the nanocasting pathway. It was found that carbon aerogels are suitable for use as templates to create monolithic mesoporous materials.

## 2. Experimental Section

**2.1. Preparation of Carbon Aerogels.** As described in a previous publication,<sup>15</sup> the carbon aerogels were prepared in aqueous solution of resorcinol (R) and formaldehyde (F) with a molar ratio of 1:2. Different from the conventionally used, slightly basic sodium carbonate (Na<sub>2</sub>CO<sub>3</sub>) as catalyst, we primarily used magnesium acetate (Mg(CH<sub>3</sub>COO)<sub>2</sub>) as catalyst with various catalyst concentrations (referred to as R/Cat, molar ratio) to prepare a series of carbon aerogels with solid contents of 30 and 40 wt %, respectively. In more detail, resorcinol (Fluka, 99%), formaldehyde (Fluka, 36.5% in water, methanol-stabilized), and magnesium acetate tetrahydrate (Fluka, 99.5%) were dissolved in deionized water under magnetic stirring to obtain a homogeneous solution. After curing (1 day at room temperature, 1 day at 50 °C, and 3 days at 90 °C), the wet gels were immersed in acetone to exchange the water inside the pores, then dried at room temperature under ambient pressure, further pyrolyzed at temperatures of up to 800 °C under argon atmosphere, and thus were transformed into carbon aerogels. The samples were denoted as CA30/*x*, CA40/*x*, respectively, wherein series CA30/*x* represents the carbon aerogels prepared with a solid content of 30 wt %, and series CA40/*x* with a solid content of 40 wt %, where *x* indicates the catalyst concentration (see Table 1).

Additionally, magnesium hydroxide (Fluka, 95%) was selected as an alternative Mg<sup>2+</sup> source for a comparison. Magnesium hydroxide is basically insoluble in water. Thus, the desired amounts of magnesium hydroxide were directly added to deionized water. After stirring and a subsequent resting phase, the supernatant clear solution, in which the Mg<sup>2+</sup> concentration was determined as 0.0018 M, was used for the synthesis of the aqueous organic gel. The synthetic procedures were essentially the same as the ones described

(16) Saliger, R.; Fischer, U.; Fricke, J. *J. Non-Cryst. Solids* **1998**, 225, 81.

(17) Tamon, H.; Ishizaka, H.; Yamamoto, T.; Suzuki, T. *Carbon* **1999**, 37, 2049.

(18) Maldonado-Hodar, F. J.; Moreno-Castilla, C.; Rivera-Utrilla, J.; Hanzawa, Y.; Yamada, Y. *Langmuir* **2000**, 16, 4367.

(19) Maldonado-Hodar, F. J.; Pérez-Cadenas, A. F.; Moreno-Castilla, C. *Carbon* **2003**, 41, 1291.

(20) Tao, Y.; Kanoh, H.; Kaneko, K. *J. Am. Chem. Soc.* **2003**, 125, 6044.

above, and the solid content was varied as 25 and 40 wt %, respectively. Carbon aerogels obtained using  $\text{Mg}(\text{OH})_2$  as catalyst were named as CA25- $\text{Mg}(\text{OH})_2$  and CA40- $\text{Mg}(\text{OH})_2$ . In addition, two more carbon aerogels were synthesized with the conventional  $\text{Na}_2\text{CO}_3$  as catalyst. The catalyst concentration was kept at  $R/\text{Cat} = 500$ , and the solid content was adjusted at 30 and 40 wt %, respectively. The obtained samples were denoted as CA30/500- $\text{Na}_2\text{CO}_3$  and CA40/500- $\text{Na}_2\text{CO}_3$ . Moreover, at a solid content of 30 wt %, resorcinol and formaldehyde were directly polycondensated without any catalyst. This carbon aerogel was denoted as CA30-NO.

To examine the pore interconnectivity, the obtained carbon aerogels were used as hard templates to synthesize, as a model system, porous silica via the nanocasting pathway. Tetraethyl orthosilicate (TEOS, 99%, Aldrich) as silica precursor was filled into the carbon aerogel pore system by impregnation. One drop of 37% concentrated hydrochloric acid was added to prompt the hydrolysis of TEOS. The impregnation step was repeated once. The silica monolith was obtained by calcination of the silica/carbon composite at 600 °C for 8 h to completely remove the carbon template.

**2.2. Characterization.** The nitrogen adsorption isotherms of all the samples were recorded with an ASAP2010 adsorption analyzer (Micromeritics) at 77 K. Prior to the sorption measurements, all the samples were degassed at 250 °C for at least 6 h. The pore sizes and pore size distributions were calculated by the BJH (Barrett–Joyner–Halenda) method from the desorption branch. Total pore volume was estimated from the amount adsorbed at  $p/p_0 = 0.99$ . Micropore volume was calculated by the  $\alpha_s$ -plot method using carbon black Cabot BP 280 as the reference.<sup>21</sup> The specific surface areas were determined by the BET method. Scanning electron microscopy (SEM) investigations were performed with a Hitachi S-3500N instrument. For transmission electron microscopy (TEM) analysis, we used a Hitachi HF2000 microscope equipped with a cold field emission gun at a beam energy of 200 kV. TG-DTA measurements for organic aerogels and carbon aerogels were carried out on Netzsch thermal analysis system. The heating rate was fixed at 5 °C/min for organic aerogels under argon and 10 °C/min for carbon aerogels under air.

### 3. Results and Discussion

In the synthesis of the carbon aerogels using magnesium acetate as catalyst, four catalyst concentrations ( $R/\text{Cat}$ , molar ratio = 50, 100, 200, and 500) were studied. Solid contents were fixed at 30 and 40 wt %, respectively. After dissolving resorcinol, formaldehyde, and magnesium acetate in deionized water, the homogeneous solution was subjected to the curing procedure described in the Experimental Section. It was found that the solution with  $R/\text{Cat} = 50$  already formed a hydrogel at 50 °C, whereas the other solutions with high  $R/\text{Cat}$  ratios do not form a gel until cured at 90 °C. The different gelation behavior will result in carbon aerogels with different frameworks. The pore structures of these carbon aerogels were characterized by nitrogen sorption isotherms, as shown in Figure 1 (solid content 30 wt %) and Figure 2 (solid content 40 wt %). Essentially, these isotherms have type IV characteristics with H1-type hysteresis loops. Samples shown in Figure 2 have larger hysteresis loops than those in Figure 1. However, most of the samples, especially

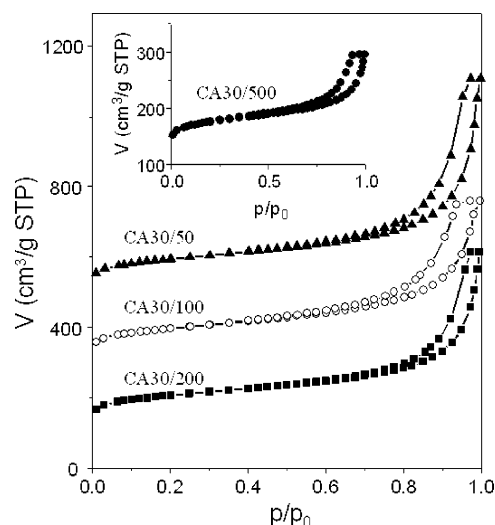


**Figure 1.** Nitrogen sorption isotherms of the carbon aerogels (solid content = 30 wt %) catalyzed by magnesium acetate (insert isotherm is of CA30/500). The isotherms of CA30/50 and CA30/100 are offset vertically by 400 and 200  $\text{cm}^3 \text{STP g}^{-1}$ , respectively.

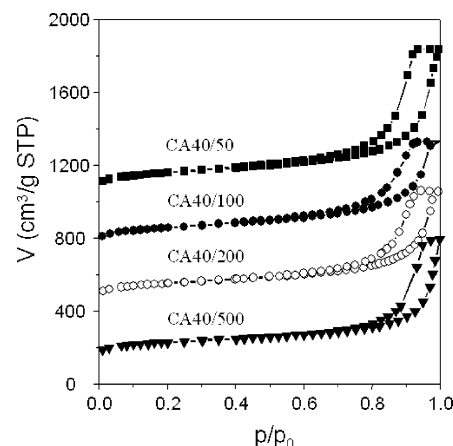


**Figure 2.** Nitrogen sorption isotherms of the carbon aerogels (solid content = 40 wt %) catalyzed by magnesium acetate. The isotherms of CA40/50, CA40/100, and CA40/200 are offset vertically by 950, 650, and 350  $\text{cm}^3 \text{STP g}^{-1}$ , respectively.

samples prepared with solid content of 30 wt %, do not reach an adsorption plateau at a relative pressure close to unity, indicating the existence of a pore system extending into the macropore regime. CA30/500 shows a low adsorption volume and a small loop compared to the other samples, implying smaller pore size and lower pore volume. Upon varying the  $R/\text{Cat}$  ratio from 50 to 500, generally the hysteresis loops become smaller and the closing points of the hysteresis loops shift to higher relative pressures. Lower catalyst concentrations thus induce formation of larger pores.

Figure 3 shows the isotherms of the carbon aerogels catalyzed by magnesium hydroxide at a solid content of 25 and 40 wt %, respectively. Interestingly, these carbon aerogels exhibit type I nitrogen sorption isotherms, suggesting the presence of a micropore system. These samples show no obvious mesoporosity, as compared with those samples catalyzed by magnesium acetate. In addition, sample CA-NO synthesized without using any catalyst also exhibits a type I isotherm, similar to those of CA25- $\text{Mg}(\text{OH})_2$  and CA40- $\text{Mg}(\text{OH})_2$ . Although sample CA-NO exhibits a similarity in the isotherms compared with CA25- $\text{Mg}(\text{OH})_2$  and

(21) Kruk, M.; Jaroniec, M.; Gadkaree, K. P. *J. Colloid Interface Sci.* **1997**, *192*, 250.



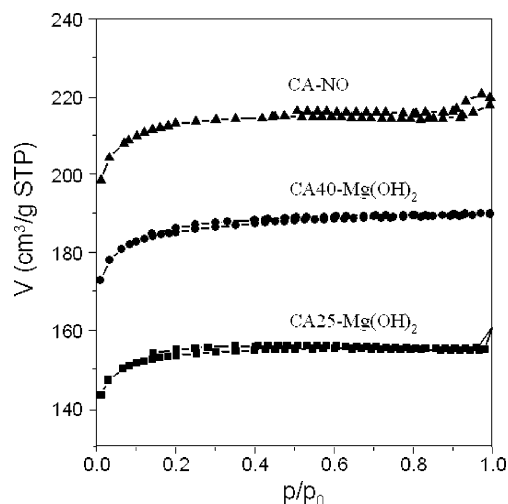


**Figure 3.** Nitrogen sorption isotherms of the carbon aerogels catalyzed by magnesium hydroxide and without catalyst. The isotherms of CA-NO and CA40-Mg(OH)<sub>2</sub> are offset vertically by 30 and 25 cm<sup>3</sup> STP g<sup>-1</sup>, respectively.

CA40-Mg(OH)<sub>2</sub>, their pore structures are still different. One very obvious difference is the fact that, during the drying step, samples CA25-Mg(OH)<sub>2</sub> and CA40-Mg(OH)<sub>2</sub> do not show any visible volume shrinkage as compared to the original hydrogel. In contrast to this, sample CA-NO shows an obvious linear shrinkage of up to 45% during the ambient pressure drying, even though the water inside the pores was exchanged against acetone to reduce the surface tension. This illustrates that the frameworks of samples CA25-Mg(OH)<sub>2</sub> and CA40-Mg(OH)<sub>2</sub> are mechanically sufficiently stable to withstand the capillary pressure, whereas the capillary stress leads to structural collapse of sample CA-NO.

For comparison, carbon aerogels were also prepared using the conventional Na<sub>2</sub>CO<sub>3</sub> catalyst under identical reaction conditions. The nitrogen sorption isotherms of such carbon aerogels are of the IV type with well-pronounced H1 hysteresis loops. At a relative pressure close to unity, the adsorption gradually reaches a plateau, which essentially reveals that no or few macropores are present in these carbon aerogels prepared with Na<sub>2</sub>CO<sub>3</sub> as catalyst.

The calculated textural parameters of all the samples are compiled in Table 1. The carbon aerogels catalyzed by magnesium acetate show comparative BET surface areas with those catalyzed by Na<sub>2</sub>CO<sub>3</sub>. However, the micropore volumes of samples catalyzed by magnesium acetate are markedly higher than those synthesized with Na<sub>2</sub>CO<sub>3</sub>, and the R/Cat ratio has a significant influence on the micropore volume. At R/Cat ratios from 50 to 500, the micropore volume gradually increases. Especially, samples CA 30/500 and CA40/500 with an R/Cat ratio of 500 have the highest micropore volume among these samples. This is also reflected by the increased ratios of  $V_{\text{mic}}/V$ . In turn, the mesopore volume decreases with increasing R/Cat ratio. Obviously, the micropore volume does not strongly depend on the solid content. However, the mesopore volume increases with the solid content, regardless of the catalyst. The pore volume of carbon aerogels synthesized with magnesium acetate is generally slightly lower than that of samples made with Na<sub>2</sub>CO<sub>3</sub>. Obviously, the pore volume can be influenced by the synthesis parameters investigated. The

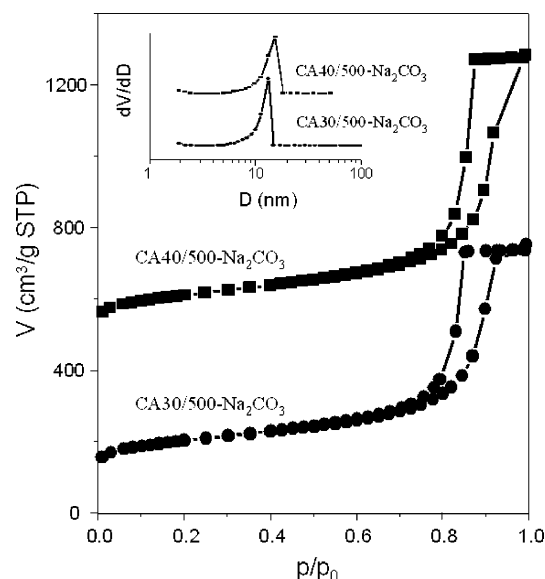


**Figure 4.** Nitrogen sorption isotherms of the carbon aerogels catalyzed by sodium carbonate. The isotherm of CA40/500-Na<sub>2</sub>CO<sub>3</sub> is offset vertically by 400 cm<sup>3</sup> STP g<sup>-1</sup>. Insert is the corresponding PSD of the carbon aerogels.

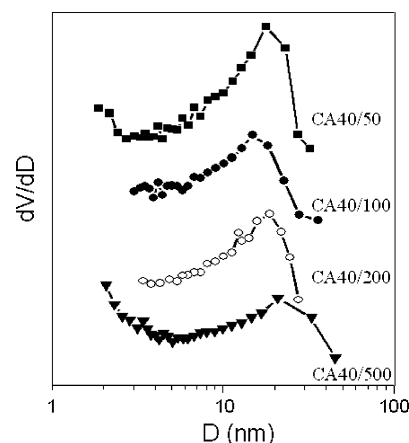


**Figure 5.** Representative PSD of the carbon aerogels catalyzed by magnesium acetate (solid content = 40 wt %).

total pore volume and the mesopore volume increase with the solid content, and a high R/Cat ratio always results in the decrease of the total pore volume, but an increase in micropore volume. However, samples CA25-Mg(OH)<sub>2</sub> and CA40-Mg(OH)<sub>2</sub>, synthesized in magnesium hydroxide solution, are essentially microporous materials since the micropore volumes are up to 92% of the total pore volume (see Table 1). Sample CA-NO which had been synthesized without catalyst shows a microporous character as well. However, the micropore volume of CA-NO is smaller than that of CA25-Mg(OH)<sub>2</sub> or CA40-Mg(OH)<sub>2</sub>. The presence of Mg(OH)<sub>2</sub> in the starting sol-gel solution results in a somewhat different pore structure for the carbon aerogels, even though only a tiny amount of Mg(OH)<sub>2</sub> is present in the aqueous solution. This different pore structure is also reflected by the different shrinkage behavior mentioned above.

The pore size distributions (PSD) of the carbon aerogels synthesized with magnesium acetate at a solid content of 40 wt % are shown in Figure 5. The carbon aerogels have a monomodal pore size distribution in the mesopore range, and the dominant pores concentrate around 20 nm. The maxima

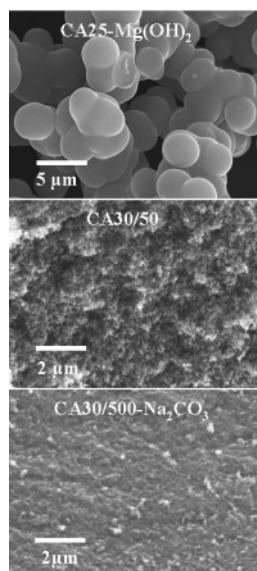


Figure 6. SEM images of selected carbon aerogels.

in the PSD curves shift to larger values with increasing R/Cat ratio. In contrast, samples catalyzed by  $\text{Na}_2\text{CO}_3$  exhibit very uniform PSDs in the range of 10–20 nm (Figure 4, insert). Furthermore, additional information regarding the porous structure can be revealed by scanning electron microscopic (SEM) and transmission electron microscopic (TEM) investigations.

The morphologies (SEM) of representative samples CA25- $\text{Mg}(\text{OH})_2$ , CA30/50, and CA30/500- $\text{Na}_2\text{CO}_3$  are shown in Figure 6. Sample CA25- $\text{Mg}(\text{OH})_2$  consists of well-pronounced spherical carbon particles with a diameter of about 3–4  $\mu\text{m}$ . Some particles coalesce through necklike structures to form the macropore space with developed pore interconnectivity. Due to this structure, such samples can maintain their monolithic shape and show almost no volume shrinkage during the ambient pressure drying process. Using this property, it may be possible to synthesize this carbon aerogel directly in a chromatography column as the stationary phase to avoid the pressure drop, for instance for high-performance liquid chromatography (HPLC). The morphology of the sample CA30/50 shows a coarser surface than that of CA30/500- $\text{Na}_2\text{CO}_3$ . No clearly visible macropores are observed for these two samples. The carbon particles tend to overlap, probably due to coalescence in the sol–gel stage. The estimated particle size of these two samples is obviously smaller than that of CA25- $\text{Mg}(\text{OH})_2$ .

TEM images of these samples are shown in Figure 7. CA25- $\text{Mg}(\text{OH})_2$  exhibits a wormlike morphology, which is related to the micropores in the carbon aerogel, as reflected by the isotherm in Figure 3. The structures of CA30/50 and CA30/500- $\text{Na}_2\text{CO}_3$  are similar to each other in the TEM images. Carbon nanoparticles with diameters of roughly 20 nm for CA30/50 and 15 nm for CA30/500- $\text{Na}_2\text{CO}_3$  form the three-dimensional network of the carbon aerogels. Thus, CA30/50 and CA30/500- $\text{Na}_2\text{CO}_3$  exhibit a structural similarity both at the nanometer length scale and on the micrometer scale. Nevertheless, examining all the carbon aerogels, their porous structure covered a wide range of properties, resulting from the different synthetic conditions.

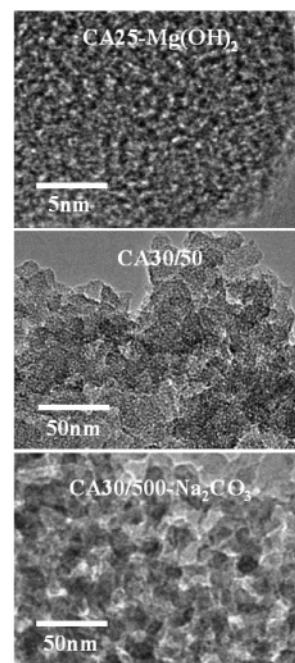


Figure 7. TEM images of selected carbon aerogels.

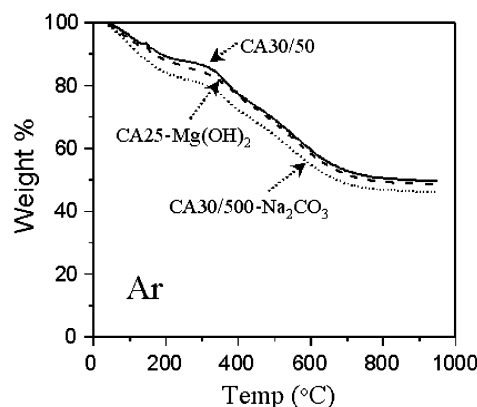
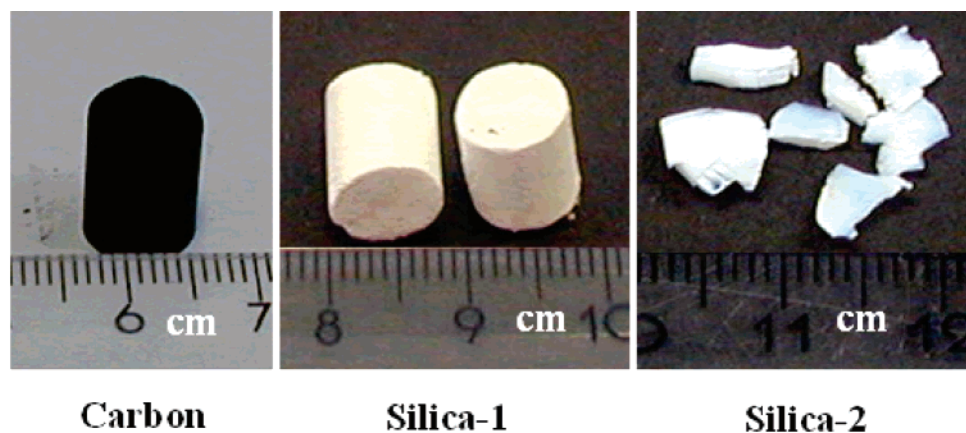


Figure 8. TG curves of organic aerogels under argon.

Elemental analyses show that organic aerogels after acetone exchange and drying contain 0.3 and 0.05 wt %  $\text{Mg}^{2+}$  in the organic precursor of CA30/50 and CA25- $\text{Mg}(\text{OH})_2$ , respectively. To investigate whether such amounts of  $\text{Mg}^{2+}$  have a pronounced influence on the final porous structure of the carbon aerogels, these two samples as well as the sample CA30/500- $\text{Na}_2\text{CO}_3$  were analyzed with thermogravimetry (TG). As shown in Figure 8, the different organic aerogels treated under argon basically show very similar pyrolysis behavior, even though they were prepared with different catalysts and solid content. Thus, the small amounts of metal ions present in the gels do not strongly alter the pyrolysis behavior, so that the differences in the textural properties can be traced back to the influence of the catalyst during the gel formation stage. The polycondensation of resorcinol and formaldehyde involves two main reactions: an addition reaction of formaldehyde to the 2-, 4-, and/or 6-position on the aromatic ring of resorcinol, which is catalyzed by bases generating more reactive resorcinol anions. This gives rise to hydroxymethyl derivatives. Subsequently, these derivatives undergo a condensation reaction to form methylene and methylene ether-bridged compounds,



**Figure 9.** Representative optical photographs of a monolithic carbon aerogel and its replicas (Silica-1 from CA25-Mg(OH)<sub>2</sub> and Silica-2 from CA30/50).

finally, to the wet gel. The catalyst used in the reaction medium is normally composed of a hydroxide anion and a metal cation. The concentration of this anion determines the imposed basic pH value, and the metal cation participates in the addition reaction in establishing the intermediate chelated form. It has been demonstrated that valence and ionic radius of the metallic cations affect the changes of species in the reaction medium. Na<sup>+</sup> and Mg<sup>2+</sup> belong to different families as a function of their behavior, which in turn can affect the morphology and porous structure of the final products.<sup>22</sup> A high charge and small ionic radius of the metal cation under basic conditions can catalyze a fast polycondensation reaction that leads to a coarse texture.<sup>23</sup> This might be the dominant reason for the different textures observed for CA30/500 and CA30/500-Na<sub>2</sub>CO<sub>3</sub>. With respect to the structural difference of the carbon aerogels catalyzed by Mg(OH)<sub>2</sub> and magnesium acetate, the initial gelation pH has a profound effect on the final properties of the carbon aerogels.<sup>24</sup> It was reported that the pore volume of carbon aerogels was determined by the pH value,<sup>25</sup> higher pH resulting in higher pore volume. Magnesium acetate leads to moderately basic solutions, and the higher the R/Cat ratio, the lower is the pH value. This is in agreement with the results listed in Table 1. Considering the narrow range of pH values which can be achieved with Mg(OH)<sub>2</sub> solution, magnesium acetate is preferable as catalyst to prepare carbon aerogels.

Recently, it has been shown that the nanocasting pathway is a very useful tool to investigate the pore interconnectivity of an inorganic porous solid, which has been intensively used in the study of mesostructured silica.<sup>6,26</sup> Accordingly, in the present study, nanocasting was employed to clarify the pore interconnectivity of the carbon aerogels. Two carbon samples, CA25-Mg(OH)<sub>2</sub> and CA30/50, with different pore structure were selected as templates. Depending on the structural stiffness and the pore connectivity of the carbon template,

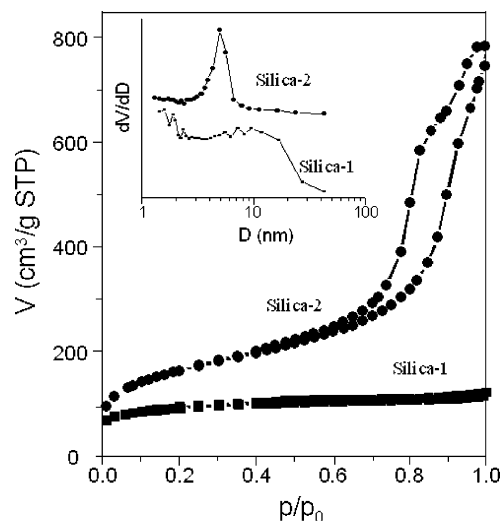


**Figure 10.** Nitrogen sorption isotherms and PSDs (insert) of silica replicas from the carbon aerogels.

the obtained silica can exhibit either a monolithic shape, replicating the original carbon template, or crack into pieces. In Figure 9, on the left side is shown a carbon aerogel monolith, in the middle is the very stable silica monolith (Silica-1) obtained from CA25-Mg(OH)<sub>2</sub>. The replica Silica-2 obtained from CA30/50 shown on the right side cannot fully maintain the original shape of the carbon template and thus breaks down into small monoliths. By cutting the silica monoliths, one can see no large holes in the middle of the monolith, indicating a homogeneous impregnation and, in turn, well-developed pore interconnectivity of the carbon aerogels. Therefore, the structural collapse in the case of Silica-2 is rather ascribed to the relatively poor structural stiffness of the carbon template rather than to its poor pore interconnectivity. During the combustion process of the carbon template, gas released can cause mechanical stress on both the silica and the carbon skeleton, leading to the partial structural collapse to release the stress. The nitrogen sorption isotherm of Silica-1 (Figure 10) shows a feature close to type I, which is almost identical to its parent carbon template (CA25-Mg(OH)<sub>2</sub>). Combining the pictures in Figure 9, one can conclude that a positive replica of CA25-Mg(OH)<sub>2</sub> via nanocasting is obtained, since the silica inherits the original shape of carbon both on the microscopic scale (pore structure) and the macroscopic scale (shape). In

(22) Moreno-Castilla, C.; Maldonado-Hodar, F. J.; Perez-Cadenas, A. F. *Langmuir* **2003**, *19*, 5650.

(23) Grenier-Loustalot, M.; Larroque, S.; Grande, D.; Grenier, P.; Bedel, D. *Polymer* **1996**, *37*, 1363.

(24) Lin, C.; Ritter, J. A. *Carbon* **1997**, *35*, 1271.

(25) Zanto, E. J.; Al-Muhtaseb, S. A.; Ritter, J. A. *Ind. Eng. Chem. Res.* **2002**, *41*, 3151.

(26) Kang, M.; Yi, S. H.; Lee, H. I.; Yie, J. E.; Kim, J. M. *Chem. Commun.* **2002**, 1944.

contrast, Silica-2 presents a type IV isotherm; the hysteresis loop is different from its parent hard template CA30/50. The closing point of the hysteresis loop shifts from high relative pressure for carbon to low relative pressure for silica, indicating the formation of Silica-2 with smaller pore size compared to the template CA30/50. The PSD of Silica-2 (insert in Figure 10) shows a monomodal distribution concentrated mainly in the range of 4–6 nm. Inspecting the isotherm more closely, one can find that it is very similar to the silica monolith synthesized by the Nakanishi method (phase transition and sol–gel process).<sup>27</sup> However, Silica-2 possesses a more uniform mesopore size and higher surface area. The formation of such uniform mesopores might be due to the templating effect from the relatively homogeneously sized carbon aerogel primary particles. As seen in Table 1, the BET surface area of Silica-2 is comparable to its parent CA30/50. However, as discussed above, their pore structures are clearly different. In carbon CA30/50, the surface area is mainly attributed to a larger portion of micropores. In contrast, the surface area of Silica-2 mainly results from its mesoporosity, since the micropore volume is only 7% of the total pore volume. This pronounced mesoporosity is caused by the interconnected silica particles templated in the pores of the carbon aerogel. In principle, without considering the structure shrinkage during a combus-

tion step, the pore size of the silica should be related to the particle size of the carbon aerogel template. In practice, this provides the possibility of preparing silica monoliths with different pore sizes by varying the particle size of the parent carbon aerogel.

#### 4. Conclusion

Monolithic carbon aerogels with well-developed porous interconnectivity can be prepared by using  $\text{Mg}^{2+}$ -containing catalysts. The nature of the metal cation and pH value of the catalyst imposed in the reaction affect the mechanism of the polycondensation reaction.  $\text{Mg}^{2+}$  with high valence and small ionic radius leads to the carbon aerogel with coarse structure. For the same metal cation, the obtained carbon aerogels exhibit micro-mesopore or micro-macropore hierarchical structures, depending on the pH value in the initial solution. Using these carbon aerogels as templates, monolithic porous silica can be obtained. This demonstrates the well-developed pore interconnectivity and the robust framework of the carbon aerogels prepared by the presented strategy.

**Acknowledgment.** We are grateful to H. Bongard for SEM measurement, B. Spliethoff for TEM measurement, and M. Schwickardi for help. The financial support from the DFG via the Leibniz-Program is gratefully acknowledged.

CM050345M

(27) Shi, Z.; Feng, Y.; Xu, L.; Da, S.; Zhang, M. *Carbon* **2003**, *41*, 2677.